Geophysical Research Letters

RESEARCH LETTER
10.1029/2020GL089469

# Intensification of Near-Surface Currents and Shear in the Eastern Arctic Ocean

**Igor V. Polyakov[1,2], Tom P. Rippeth[3], Ilker Fer[4], Till M. Baumann[1], Eddy C. Carmack[5], Vladimir V. Ivanov[6,7], Markus Janout[8], Laurie Padman[9], Andrey V. Pnyushkov[6], and Robert Rember[6]**

[1]International Arctic Research Center and College of Natural Science and Mathematics, University of Alaska Fairbanks, Fairbanks, AK, USA, [2]Finnish Meteorological Institute, Helsinki, Finland, [3]School of Ocean Sciences, Bangor University, Menai Bridge, UK, [4]Geophysical Institute, University of Bergen and Bjerknes Centre for Climate Research, Bergen, Norway, [5]Institute of Ocean Sciences, Fisheries and Oceans Canada, Sidney, BC, Canada, [6]International Arctic Research Center, University of Alaska Fairbanks, Fairbanks, AK, USA, [7]Geography Department, Lomonosov Moscow State University, Moscow, Russia, [8]Alfred Wegener Institute Helmholtz Centre for Polar and Marine Research, Bremerhaven, Germany, [9]Earth and Space Research, Corvallis, OR, USA

**Abstract** A 15-year (2004–2018) record of mooring observations from the upper 50 m ocean in the eastern Eurasian Basin reveals increased current speeds and shear, associated with an increasing coupling between wind, ice, and oceanic currents and their vertical shear over 2004–2018, particularly in summer. Substantial increases in both current speeds and shears in the upper 50 m are dominated by a two times amplification of currents in the semidiurnal band, which includes tides and wind-forced near-inertial oscillations. For the first time the strengthened upper ocean currents and shear are observed to coincide with weakening stratification. This coupling links the Atlantic Water heat to the sea ice, a consequence of which would be reducing regional sea ice volume. These results point to a new positive feedback mechanism in which reduced sea ice extent facilitates more energetic inertial oscillations and associated upper-ocean shear, thus leading in enhanced ventilation of the Atlantic water.

**Plain Language Summary** Previous studies demonstrated that in recent years density gradients above the warm and salty intermediate (~150–900 m) water of Atlantic origin in the eastern Arctic Ocean have weakened, allowing stronger upward transport heat to the bottom of the sea ice. Using mooring observations, we show that this weakening of stratification has been accompanied by stronger upper-ocean currents and their vertical shear and by increasing coupling between the wind and sea ice with upper ocean currents and shear. Most of this enhanced energy and shear is in the semidiurnal band, which includes baroclinic tides and wind-driven inertial oscillations. The increased shear together with the weakening stratification indicate a greater potential for shear-driven turbulent mixing. We propose a new process, the ice/ocean-heat positive feedback, that can accelerate current sea ice loss and impede the rate of recovery of eastern Arctic sea ice even if large-scale climate warming conditions relax.

**Key Points:**
- Currents and associated shear in the upper 50 m in the eastern Eurasian Basin are increased in the 2010s
- Increased currents and shear are dominated by accelerating currents in the semidiurnal (inertial and tidal) band
- There was an increasing coupling between wind, ice, and oceanic currents in the eastern Eurasian Basin over 2004–2018

**Supporting Information:**
- Supporting Information S1

**Correspondence to:**
I. V. Polyakov,
ivpolyakov@alaska.edu

**Citation:**
Polyakov, I. V., Rippeth, T. P., Fer, I., Baumann, T. M., Carmack, E. C., Ivanov, V. V., et al. (2020). Intensification of near-surface currents and shear in the Eastern Arctic Ocean. *Geophysical Research Letters*, *46*, e2020GL089469. https://doi.org/10.1029/2020GL089469

Received 26 JUN 2020
Accepted 29 JUL 2020
Accepted article online 4 AUG 2020



## 1. Introduction

Throughout much of the Arctic Ocean layers of colder water isolates the sea surface from warm (temperature >0°C) and salty water of Atlantic origin (Atlantic Water, AW), which is transported throughout the Arctic Ocean at intermediate depths (~150–900 m) as topographically steered boundary currents (e.g., Aagaard, 1989; Rudels et al., 1994). The AW holds enough heat to melt Arctic sea ice several times over but is separated from the near-freezing, and relatively fresh water in the Arctic Ocean surface mixed layer, by a cold halocline layer which has a negligible vertical temperature gradient but a large salinity gradient. The associated density gradient impedes vertical mixing of AW heat upward to the sea ice (e.g., Fer, 2009; Rudels et al., 1996).

In the absence of significant shear-driven mixing, the vertical structure of cooler and fresher halocline water overlying the warmer and saltier AW facilitates double diffusive convection which mediates vertical heat fluxes across the lower halocline into the seasonal convective layer (Carmack et al., 2015). Double diffusion is driven by the different molecular diffusivities of heat and salt and is evident in vertical hydrographic profiles as multiple layers of near-uniform temperature and salinity that are separated by strong-gradient, thin

interfaces. These "thermohaline staircases" have been found over a large portion of the Arctic Ocean in the lower halocline water above the depth of maximum temperature in the AW layer (e.g., Guthrie et al., 2017; Polyakov et al., 2019; Shibley et al., 2017), laterally coherent for more than 800 km in the Canada Basin (Timmermans et al., 2008) and for more than 1,000 km in the Eurasian Basin (EB, Polyakov et al., 2019). In the presence of the staircases, the vertical heat flux out of the AW is limited to between O(0.1) $W/m^2$ in the central basins (Guthrie et al., 2015; Padman & Dillon, 1987; Sirevaag & Fer, 2012) and O(1) $W/m^2$ over the Laptev Sea slope (Lenn et al., 2009; Polyakov et al., 2012, 2019).

It is long established that the influence of the wind in driving mixing is significantly enhanced in open water compared to under ice through the generation of inertial oscillations in the upper ocean, with associated shear leading to shear instability and turbulent mixing (Lenn et al., 2011; Rainville & Woodgate, 2009). This led to the idea that the decline of seasonal sea ice area would result in increased mixing by the wind, thereby increasing the influence of AW in melting the sea ice (a positive feedback). However, the influence of the inertial oscillations is restricted to the upper ocean. For example, microstructure measurements made in the ice-free Canada Basin during the 2012 "perfect storm" show that while there is significantly enhanced turbulence in the upper 50 m of the water column in response to the storm, the AW heat remained isolated by the strongly stratified halocline, across which thermohaline staircase structures persisted (Lincoln et al., 2016).

In contrast, shear instabilities drive AW heat fluxes of up to 50 $W/m^2$ in the upper ocean in the western Nansen Basin near sloping topography (Carmack et al., 2015; Fer et al., 2010; Padman & Dillon, 1991; Rippeth et al., 2015), greatly diminishing the influence of the halocline and in consequence leading to a locally increasing the influence of AW heat on the sea ice extent.

In the eastern (east of 70°E) EB the halocline (60–150 m) includes the cold halocline layer and lower halocline water associated with strong vertical temperature and salinity gradients directly above the AW layer. The eastern EB halocline has become warmer and saltier since the 1970s, with a coincident weakening in stratification (Polyakov et al., 2010; Steele & Boyd, 1998). By the mid-2010s, increased AW heat fluxes were found to affect sea ice loss in the eastern EB, with the disappearance of the cold halocline layer observed during the winters of 2013–2015 (Polyakov et al., 2017). These changes made this region structurally similar to the western (west of 70°E) EB, which is closer to the AW source in Fram Strait. The combination of weaker stratification and shoaling of the AW, coupled with net loss in sea ice, has allowed progressively deeper winter ventilation and larger upward AW heat fluxes in the eastern EB (Polyakov et al., 2017). This so-called "atlantification" represents a transition toward a new Arctic climate state, in which AW heat is exerting a substantially increased influence on the seasonal freeze/melt freshwater cycle, with a trend toward reduced sea ice volume.

The aim of this paper is to examine the impact of the atlantification in the eastern EB on time varying currents in the upper ocean, and by implication mixing. To this end, we present a unique 15-year time series of upper ocean currents from an array of moorings stretching from the shelf break in the eastern EB to the basin interior. The data set is analyzed to isolate time varying currents in the inertial-tidal band which are then compared to local wind conditions and sea ice state to examine the relationship between the changing environmental conditions and the currents.

## 2. Data

### 2.1. Mooring ADCP Measurement

We use observations of ocean currents from moorings deployed in the eastern EB from 2004 to 2018; see Figure 1a for locations and Table 1 for deployment periods and instruments. The longest record is from the $M1_4$ mooring site, with several collocated moorings deployed and recovered annually prior to 2009, and longer-duration deployments after that.

During 2013–2018, moorings were deployed as a transect ($M1_1$ to $M1_6$) along 126°E from the upper continental slope (250 m isobath) to the 3,400 m isobath in the Nansen Basin (Figure 1). The area bordered by the $M1_1$ and $M1_3$ moorings, a ~70 km-wide slope segment, is occupied by the along-slope topographically steered boundary current. Averaged over 2013–2015, the maximum current speed was ~11 cm/s at the shallowest mooring $M1_1$, with only ~0.5 cm/s at moorings $M1_5$ and $M1_6$ (Pnyushkov et al., 2015, 2018, Figure 1c).

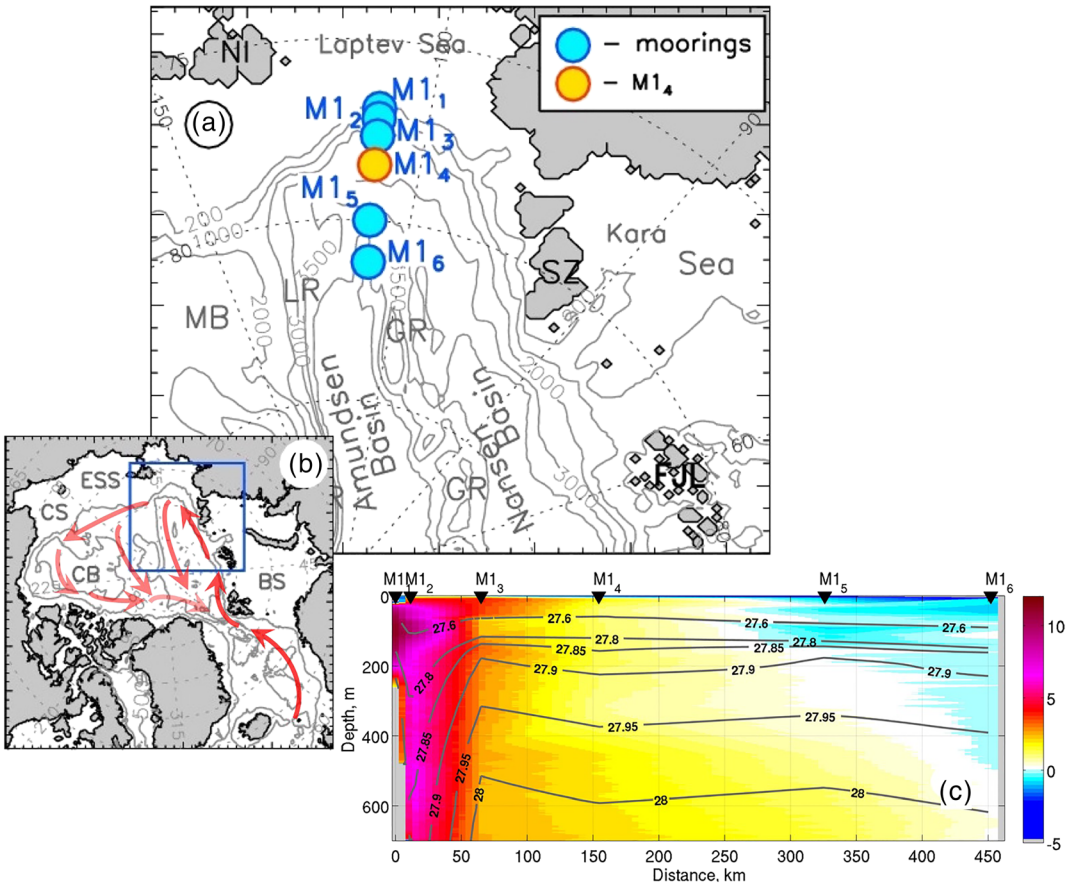


**Figure 1.** (a) Map showing the positions of moorings and ITP-36 buoy reported in this study. The Gakkel Ridge (GR) divides the Eurasian Basin (EB) into the Nansen Basin and the Amundsen Basin. The Lomonosov Ridge (LR), Novosibirskiye Islands (NI), Severnaya Zemlya (SZ), Franz Joseph Land (FJL), and Makarov Basin (MB) are indicated. Gray solid lines show depth in meters. (b) Map of larger area with the position of panel (a) indicated by the blue box. The Canada Basin (CB), Chukchi Sea (CS), East Siberian Sea (ESS), and Barents Sea (BS) are shown. (c) Distribution of the mean eastward velocity (cm/s, color) along the 126°E mooring line in 2013–2015; gray contours show mean potential density averaged over the same period (from Pnyushkov et al., 2018).

Seasonal cross-slope displacements of the boundary current were only observed over the upper slope ($M1_1$ and $M1_2$ moorings); see Baumann et al. (2018).

Most moorings used in this analysis included upward-looking 300-kHz Acoustic Doppler Current Profilers (ADCP, Teledyne RD Instruments) targeting the upper 50–60 m of the water column (Table 1). ADCPs

**Table 1**
*Summary of Upper Ocean Current Measurement Near the $M1_4$ Mooring Location*

| Mooring | Latitude (N) longitude (E) | Depth (m) | Instruments | Depth range (m) | Beginning of record | End of record |
|---|---|---|---|---|---|---|
| M1c | 78 26.637<br>125 40.194 | 2,690 | ADCP | 5–50 | 09/14/2004 | 09/15/2005 |
| M1e | 78 25.940<br>125 43.419 | 2,692 | ADCP | 5–57 | 09/02/2006 | 09/18/2007 |
| M1g | 78 25.735<br>125 28.527 | 2,765 | ADCP | 20–130 | 10/18/2008 | 06/16/2010 |
| $M1_4$ | 78 27.543<br>125 53.758 | 2,721 | ADCP | 5–55 | 09/05/2013 | 09/19/2015 |
| $M1_4$ | 78 28.084<br>125 57.679 | 2,700 | ADCP | 5–30 | 09/21/2015 09/21/2015 | 09/18/2018 09/18/2018 |

*Note*. Mooring names follow the original NABOS mooring names. Dates are in the format of month/day/year.

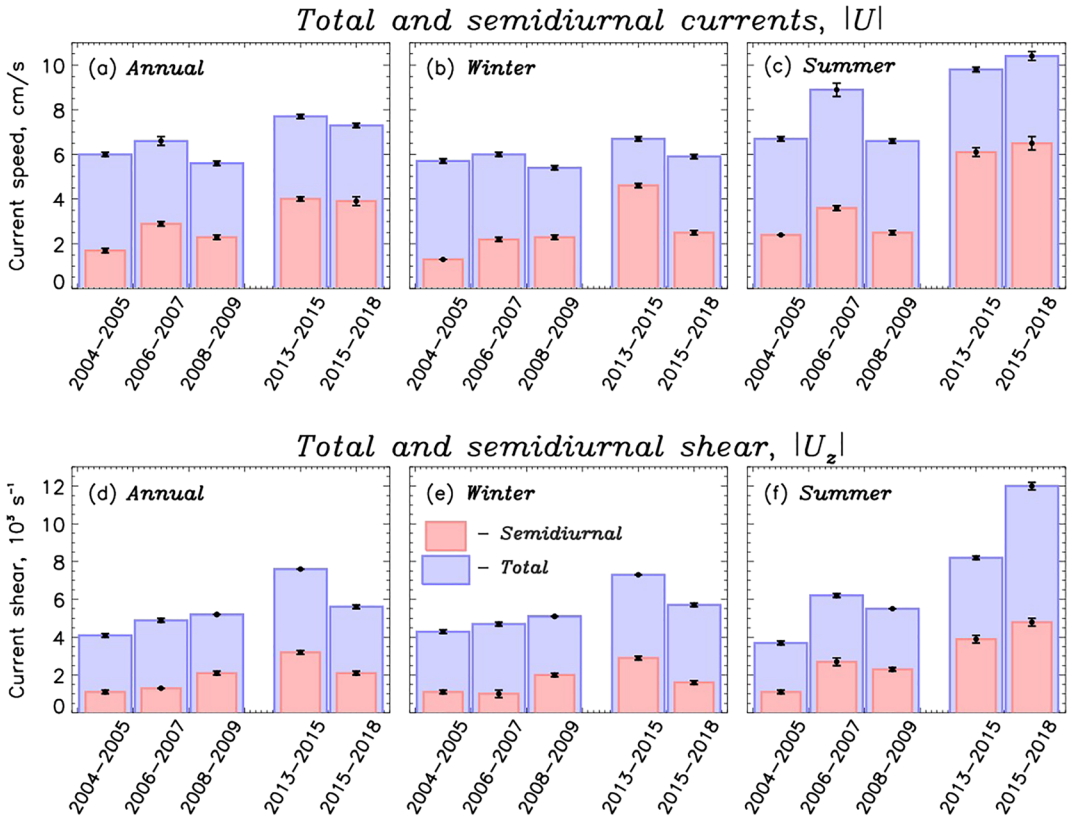


**Figure 2.** Temporal changes in total (blue) and semidiurnal-band (red) currents and their shear from 2004 to 2018 in the upper 50 m. Estimates of (a, d) annual (January–December), (b, e) winter (November–July), and (c, f) summer (August–October) for mean current speed |**U**| and vertical shear of horizontal currents $|\mathbf{U}_z|$, respectively, at the $M1_4$ mooring location. Statistical significance of means (error bars) is shown at the 95% confidence level.

provided current velocities, averaged over 2-m (prior to 2013) or 4-m (after 2013) vertical cells, with 1-hr time resolution. The manufacturer's estimates for 300-kHz ADCP accuracies are 0.5% of measured speed and 2° for current direction.

### 2.2. Winds

Daily 10-m wind output with a spatial resolution of 0.75° from the European Centre for Medium-Range Weather Forecasts reanalysis ERA-Interim (34) was used to evaluate the wind speed at the mooring locations.

### 2.3. Sea Ice Concentrations

Daily-averaged SMMR, SSM/I, SSMIS satellite observations of sea ice concentrations for 2004–2015 (NASA team algorithm; available from ftp://sidads.colorado.edu/pub/DATASETS/nsidc0051_gsfc_nasateam_seaice/final-gsfc/north/daily/) are the primary data set used to estimate ice conditions at EB mooring locations. This data set is provided on a polar stereographic grid with a 25-km spatial resolution.

## 3. Methods

### 3.1. Calculating Vertical Shear of Horizontal Currents

We filtered higher resolution 2 m ADCP vertical profiles collected prior to 2013 with a running-mean filter to reduce resolution to 4 m, equivalent to the 2013–2018 ADCP observations. The vertical shear was calculated every hour using gradients over 4 m vertical scale.

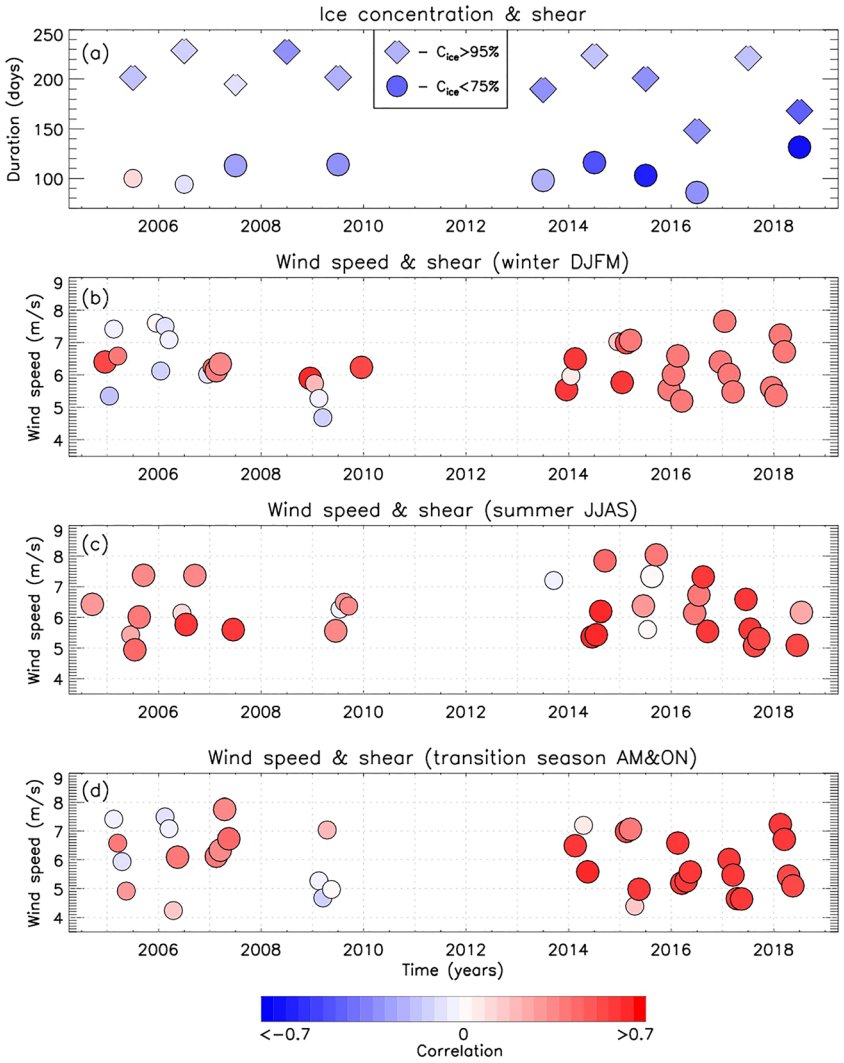


**Figure 3.** Increasing coupling between wind and sea ice forcing and ocean currents and their shear. (a) Total duration when sea ice concentration ($C_{ice}$) was less than 75% (circles) and greater than 95% (diamonds) and correlations (color) between $C_{ice}$ and current shear averaged over these two periods. (b–d) Monthly mean wind speed and correlations (color) between wind speed and current shear in (b) winter, (c) summer, and (d) transition season. All correlations are computed using daily data and 30-day running window. Statistically significant correlations are marked by larger circles. Correlation patterns for |**U**| are identical to patterns for shear (a, b) and are not shown here.

### 3.2. Cross-Correlation Analysis

Cross-correlation analysis between wind and sea ice forcing and ocean currents and shear is based on daily data. Thirty-day running window is used to calculate correlations for each specific day which were then averaged to obtain monthly estimates. The typical number of data points used for correlation analysis of summer (<75%) and winter (>95%) sea ice concentration and currents and shear was *O*(110) and *O*(200), respectively.

## 4. Results

### 4.1. Amplification of Upper-Ocean Currents and Shear in the Eastern EB

The original hourly ADCP records of total current speed (|**U**|) and shear (|$\mathbf{U_z}$|) in the upper ~30–50 m layer are shown in supporting information Figure S1. Annual, winter (November–July), and summer (August–October) data are shown in Figure 2. The mean value of |**U**| for each mooring deployment period

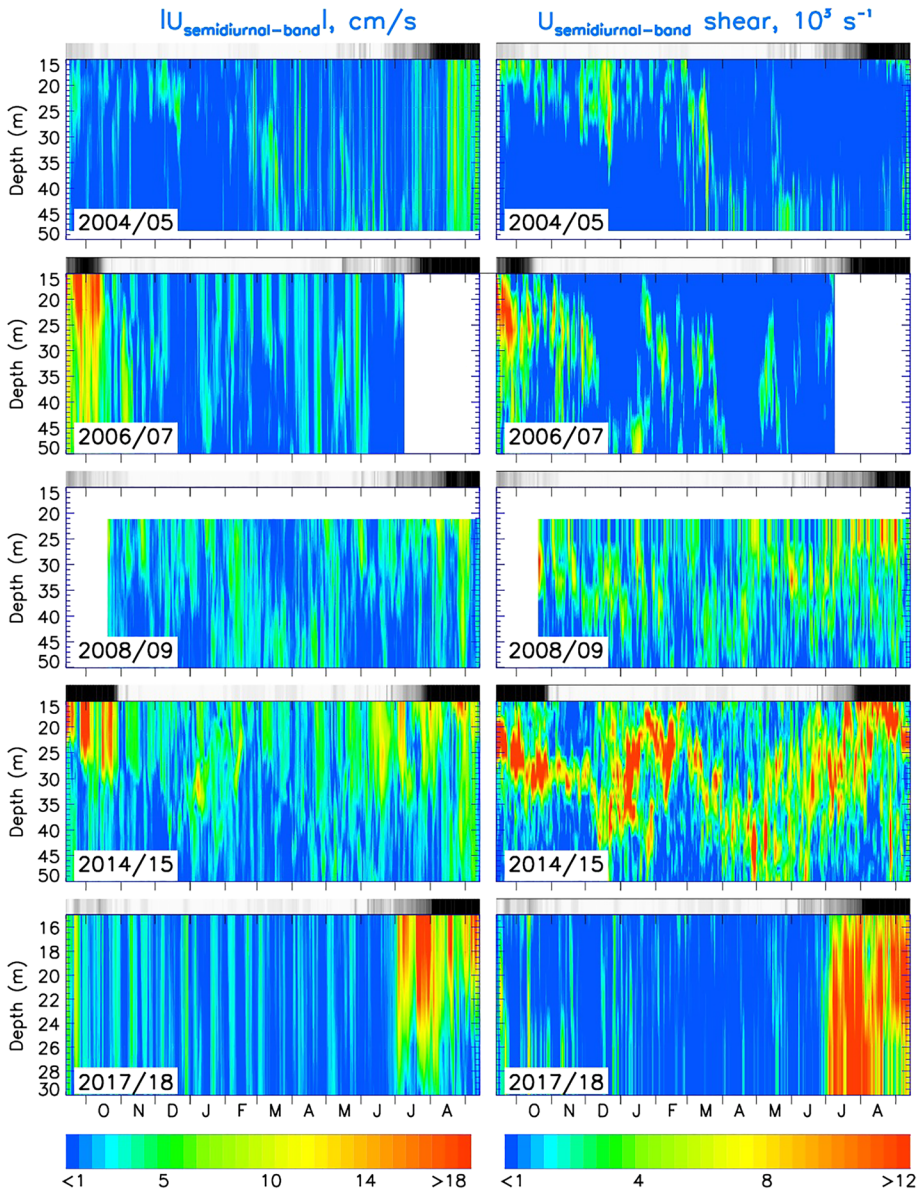


**Figure 4.** Annual records spanning 2004–2005 through to 2017–2018, showing the magnitude of the semidiurnal-band (left) and associated shear (right) at the $M1_4$ mooring location (see Figure 1a) as a function of time and depth. White segments show missing data. Black-gray-white bar over each panel shows daily sea ice concentration between 0% (black) and 100% (white) with linear color scale in between. Note different vertical scale used for the 2017–2018 panel.

increased by about 20%, from 6.0 ± 0.1 cm/s in 2004–2007 to 7.3 ± 0.1 cm/s in 2013–2018 (Figure 2a). Much of this increase occurred in summer (August–October) with the intensification particularly prominent in 2009–2018 (Figure 2c). There is no evident change of $|\mathbf{U}|$ over the same years in winter (Figure 2b). These results are consistent with findings of increased mobility of sea ice and geostrophic currents in recent decades (e.g., Armitage et al., 2017; Kwok et al., 2013; Rampal et al., 2009). Shear ($|\mathbf{U_z}|$) in the upper 50 m has increased by about 40%, for annual values, and ~90%, for summer values, between 2004–2007 and 2013–2018 (Figures 2d–2f).

This amplification of the upper ocean $|\mathbf{U}|$ and $|\mathbf{U_z}|$ is associated with increasing coupling between wind, ice, and oceanic currents, as evidenced by increase, in time, of (a) the negative correlation between sea ice concentration and shear and (b) the positive correlation between wind speed and shear at the $M1_4$ mooring site over 2004–2018 (Figure 3). During this period, annually averaged sea ice concentration in the eastern EB

decreased by $-0.5 \pm 0.2\%$ per year (not shown). This decline is dominated by the sea ice retreat in the summer ($-0.6 \pm 0.4\%$ per year in September) with a more modest reduction in winter concentration ($-0.10 \pm 0.04\%$ per year in April). Intensification of coupling expressed as an increase in time of the negative correlations between the sea ice concentration and currents and their shear is better pronounced in summer than in winter (Figure 3a), consistent with Rainville and Woodgate (2009). Over this period, there was no significant trend in wind speed. Analysis of seasonal changes of coupling between wind speed and $|\mathbf{U}|$ and $|\mathbf{U_z}|$ reveal increasingly strong correlations in summer and, especially, during the sea ice transition seasons; however, in winter the increase of coupling is not as strong. This is consistent with the lack of significant increase in the overall winter-average shear (Figure 2e).

For the 15-year duration of the mooring observations, the increase in $|\mathbf{U}|$ in the upper 50 m of the water column is almost completely accounted for by an increase in currents in a frequency band centered near two cycles per day (Figure 2). This band includes the semidiurnal tides and, at these latitudes, inertial oscillations forced by changes in wind stress. This frequency band often dominates Arctic Ocean current and sea ice velocity variability (e.g., Dosser & Rainville, 2016; Gimbert et al., 2012; Lenn et al., 2011; Rainville & Woodgate, 2009).

We band-pass filtered the observed hourly current records to isolate oscillations with periods 10–14 hr and so retain only the semidiurnal-band current (SBC). Near-surface SBCs and shears increased by a factor of 2 between 2004–2005 and 2015–2018 (Figures 2 and 3). The SBCs increased in both open water (summer) and high sea-ice concentration conditions (winter). The largest annual-averaged SBCs were measured over the period 2013–2018 (Figure 2a). Winter SBCs declined from 2013–2015 to 2015–2018 (Figure 2b); however, summer values increased slightly during the same period (Figure 2c), indicating interannual variability in seasonal conditions. The consistency of changes in SBCs and SBC shears since 2013 at all mooring locations (Figure S2) indicate that the reported changes of upper ocean currents are temporal and not due to the geographic position of the measurements (see, also, discussion in Polyakov et al., 2017).

The largest SBCs and shears in the 10–50 m layer correspond to the ice-free season in all years presented (Figures 4 and S2), consistent with previous observations showing that compact sea ice cover dampens the semidiurnal ocean response to wind forcing (Lenn et al., 2011; Lincoln et al., 2016; Rainville & Woodgate, 2009). However, there were significant SBCs and SBC shears even under winter sea ice conditions between 2008 and 2018, in contrast to a lack of significant SBC energy from the earlier winters of 2004–2007.

## 5. Discussion

Measurements of currents from a 15-year duration mooring record in the eastern EB of the Arctic Ocean demonstrate that the previously identified weakening of stratification in the halocline (e.g., Polyakov et al., 2017, 2018) has been accompanied by increased upper-ocean current speeds and associated current shear. Most of this increased energy and shear is in the semidiurnal band, which includes baroclinic tides and wind-driven inertial oscillations, with little change of mean along-slope water transport (Pnyushkov et al., 2018). The increased shear presented in this research together with the weakening stratification identified earlier indicate a greater potential for shear-driven turbulent mixing, consistent with the recent transition in sea ice and upper ocean state to conditions previously unique to the western Nansen Basin (Polyakov et al., 2017).

We hypothesize that this increased coupling between AW heat and the sea ice may lead to a positive feedback between reduced sea ice and higher mixing rates as the longer periods and increased areal extent of open water facilitate more energetic wind-driven inertial oscillations (and, potentially, less damping of baroclinic tidal currents) and associated upper-ocean shear coinciding with weakening halocline stratification.

As sea ice declines, a new Arctic state is emerging which, due to the positive feedback mechanism outlined above, may be pushing the system toward a tipping point. Both observations (e.g., Polyakov et al., 2005; Schauer et al., 2004; Woodgate et al., 2001) and modeling results (Karcher et al., 2003) indicate that AW fluctuations in the Arctic Ocean interior are also linked to the highly variable nature of the AW inflows, with abrupt cooling/warming events. In future, such a pulse of AW may lead to a permanently Atlantic-dominated state in this region, wherein the hydrographic structure of the halocline no longer insulates the AW heat from the sea ice, even during later periods of weaker AW heat input. This transition of the

eastern Arctic Ocean toward a new state points to the need for models including the region to resolve changing AW inputs as well as sensitivity of the time varying currents to the evolving stratification and sea ice state.

## Data Availability Statement

All data are available online (Polyakov, 2016, 2019). All mooring data used in this study are available online (https://arcticdata.io/catalog/#view/arctic-data).

**Acknowledgments**
The oceanographic observations in the eastern EB and Laptev Sea were conducted under the framework of the NABOS project with support from NSF (grants AON-1203473, AON-1338948, and AON-1203146). Analyses presented in this paper are supported by NSF grants 1249133, 1249182, 1708424, and 1708427. The contributions from TPR and MAJ were supported by PEANUTS (NE/R01275X/1 and 03F0804A), part of the Changing Arctic Ocean programme, jointly funded by the UKRI Natural Environment Research Council (NERC) and the German Federal Ministry of Education and Research (BMBF). IF was supported by the Research Council of Norway through the AROMA project (294396).

## References

Aagaard, K. (1989). A synthesis of Arctic Ocean circulation. *Rapp. P.-v. Reun. Cons. Int. Explor. Mer.*, *188*, 11–22. https://doi.org/10.4095/126774

Armitage, T. W. K., Bacon, S., Ridout, A. L., Petty, A. A., Wolbach, S., & Tsamados, M. (2017). Arctic Ocean surface geostrophic circulation 2003-2014. *The Cryosphere*, *11*, 1767–1780. https://doi.org/10.5194/tc-2017-22

Baumann, T. M., Polyakov, I. V., Pnyushkov, A. V., Rember, R., Ivanov, V. V., Alkire, M. B., et al. (2018). On the seasonal cycles observed at the continental slope of the eastern Eurasian Basin of the Arctic Ocean. *Journal of Physical Oceanography*, *48*(7), 1451–1470. https://doi.org/10.1175/JPO-D-17-0163.1

Carmack, E. C., Polyakov, I. V., Padman, L., Fer, I., Hunke, E., Hutchings, J., et al. (2015). Toward quantifying the increasing role of oceanic heat in sea ice loss in the new Arctic. *BAMS*, *96*(12), 2079–2105. https://doi.org/10.1175/BAMS-D-13-00177.1

Dosser, H., & Rainville, L. (2016). Dynamics of the changing near-inertial wave field in the Arctic Ocean. *Journal of Physical Oceanography*, *46*(2), 395–415. https://doi.org/10.1175/JPO-D-15-0056.1

Fer, I. (2009). Weak vertical diffusion allows maintenance of cold halocline in the central Arctic. *Atmospheric and Oceanic Science Letters*, *2*, 148–152. https://doi.org/10.1080/16742834.2009.11446789

Fer, I., Skogseth, R., & Geyer, F. (2010). Internal waves and mixing in the marginal ice zone near the Yermak Plateau. *Journal of Physical Oceanography*, *40*(7), 1613–1630. https://doi.org/10.1175/2010JPO4371.1

Gimbert, F., Marsan, D., Weiss, J., Jourdain, N. C., & Barnier, B. (2012). Sea ice inertial oscillations in the Arctic Basin. *The Cryosphere.*, *6*(5), 1187–1201. https://doi.org/10.5194/tc-6-1187-2012

Guthrie, J., Fer, I., & Morison, J. (2015). Observational validation of the diffusive convection flux laws in the Amundsen Basin, Arctic Ocean. *Journal of Geophysical Research: Oceans*, *120*, 7880–7896. https://doi.org/10.1002/2015JC010884

Guthrie, J., Fer, I., & Morison, J. (2017). Thermohaline staircases in the Amundsen Basin: Possible disruption by shear and mixing. *Journal of Geophysical Research: Oceans*, *122*, 7767–7782. https://doi.org/10.1002/2017JC012993

Karcher, M. J., Gerdes, R., Kauker, F., & Koberle, C. (2003). Arctic warming: Evolution and spreading of the 1990s warm event in the Nordic seas and the Arctic Ocean. *Journal of Geophysical Research*, *108*(C2), 3034. https://doi.org/10.1029/2001JC001265

Kwok, R., Spreen, G., & Pang, S. (2013). Arctic sea ice circulation and drift speed: Decadal trends and ocean currents. *Journal of Geophysical Research: Oceans*, *118*, 2408–2425. https://doi.org/10.1002/jgrc.20191

Lenn, Y.-D., Rippeth, T. P., Old, C. P., Bacon, S., Polyakov, I., Ivanov, V., & Hollemann, J. A. (2011). Intermittent intense turbulent mixing under ice in the Arctic Halocline of the Laptev Self Sea. *Journal of Physical Oceanography*, *43*(3), 531–547. https://doi.org/10.1175/2010jpo4425.1

Lenn, Y.-D., Wiles, P., Torres-Valdes, S., Abrahamsen, E., Rippeth, T., Simpson, J. H., et al. (2009). Vertical mixing at intermediate depths in the Arctic boundary current. *Geophysical Research Letters*, *36*, L05601. https://doi.org/10.1029/2008GL036792

Lincoln, B. J., Rippeth, T. P., Lenn, Y.-D., Timmermans, M. L., Williams, W. J., & Bacon, S. (2016). Wind-driven mixing at intermediate depths in an ice-free Arctic Ocean. *Geophysical Research Letters*, *43*, 9749–9756. https://doi.org/10.1002/2016GL070454

Padman, L., & Dillon, T. M. (1987). Vertical heat fluxes through the Beaufort Sea thermohaline staircase. *Journal of Geophysical Research*, *92*(C10), 10799. https://doi.org/10.1029/JC092iC10p10799

Padman, L., & Dillon, T. M. (1991). Turbulent mixing near the Yermak Plateau during the coordinated Eastern Arctic Experiment. *Journal of Geophysical Research*, *96*(C3), 4769–4782. https://doi.org/10.1029/90JC02260

Pnyushkov, A., Polyakov, I. V., Ivanov, V., Aksenov, Y., Coward, A., Janout, M., & Rabe, B. (2015). Structure and variability of the boundary current in the Eurasian Basin of the Arctic Ocean. *Deep Sea Research, Part I*, *101*(7), 80–97. https://doi.org/10.1016/j.dsr.2015.03.001

Pnyushkov, A. V., Polyakov, I. V., Rember, R., Ivanov, V. V., Alkire, M. B., Ashik, I. M., et al. (2018). Heat, salt, and volume transports in the eastern Eurasian Basin of the Arctic Ocean from 2 years of mooring observations. *Ocean Science*, *14*(6), 1349–1371. https://doi.org/10.5194/os-14-1349-2018

Polyakov, I. V. (2016). NABOS II - Mooring Data 2013-2015. Arctic Data Center, https://doi.org/10.18739/A2N37R

Polyakov, I. V. (2019). Acoustic Dopper Current Profiler (ADCP) from moorings taken in the Eurasian and Makarov basins, Arctic Ocean, 2015-2018. Arctic Data Center. https://doi.org/10.18739/A2HT2GB80

Polyakov, I. V., Beszczynska, A., Carmack, E. C., Dmitrenko, I. A., Fahrbach, E., Frolov, I. E., et al. (2005). One more step toward a warmer Arctic. *Geophysical Research Letters*, *32*, L17605. https://doi.org/10.1029/2005GL023740

Polyakov, I. V., Padman, L., Lenn, Y.-D., Pnyushkov, A. V., Rember, R., & Ivanov, V. V. (2019). Eastern Arctic Ocean diapycnal heat fluxes through large double-diffusive steps. *Journal of Physical Oceanography*, *49*, 227–246. https://doi.org/10.1175/JPO-D-18-0080.1

Polyakov, I. V., Pnyushkov, A. V., Alkire, M., Ashik, I. M., Baumann, T., Carmack, E., et al. (2017). Greater role for Atlantic inflows on sea-ice loss in the Eurasian Basin of the Arctic Ocean. *Science*, *356*(6335), 285–291. https://doi.org/10.1126/science.aai8204

Polyakov, I. V., Pnyushkov, A. V., & Carmack, E. C. (2018). Stability of the arctic halocline: A new indicator of arctic climate change. *Environmental Research Letters*, *13*, 125008. https://doi.org/10.1088/1748-9326/aaec1e

Polyakov, I. V., Pnyushkov, A. V., Rember, R., Ivanov, V. V., Lenn, Y.-D., Padman, L., & Carmack, E. C. (2012). Mooring-based observations of the double-diffusive staircases over the Laptev Sea slope. *Journal of Physical Oceanography*, *42*, 95–109. https://doi.org/10.1175/2011JPO4606.1

Polyakov, I. V., Timokhov, L. A., Alexeev, V. A., Bacon, S., Dmitrenko, I. A., Fortier, L., et al. (2010). Arctic Ocean warming reduces polar ice cap. *Journal of Physical Oceanography*, *40*, 2743–2756. https://doi.org/10.1175/2010JPO4339.1

Rainville, L., & Woodgate, R. A. (2009). Observations of internal wave generation in the seasonally ice-free Arctic. *Geophysical Research Letters*, *36*, L23604. https://doi.org/10.1029/2009GL041291

Rampal, P., Weiss, J., & Marsan, D. (2009). Positive trend in the mean speed and deformation rate of Arctic sea ice, 1979–2007. *Journal of Geophysical Research*, *114*, C05013. https://doi.org/10.1029/2008jc005066

Rippeth, T. P., Lincoln, B. J., Lenn, Y.-D., Green, J. M., Sundfjord, A., & Bacon, S. (2015). Tide-mediated warming of Arctic halocline by Atlantic heat fluxes over rough topography. *Nature Geoscience*, *8*, 191–194. https://doi.org/10.1038/ngeo2350

Rudels, B., Anderson, L. G., & Jones, E. P. (1996). Formation and evolution of the surface mixed layer and halocline of the Arctic Ocean. *Journal of Geophysical Research*, *101*(C4), 8807–8821. https://doi.org/10.1029/96JC00143

Rudels, B., Jones, E. P., Anderson, L. G., & Kattner, G. (1994). On the intermediate depth waters of the Arctic Ocean. In O. M. Johannessen, R. D. Muench, & J. E. Overland (Eds.), *The Polar Oceans and Their Role in Shaping the Global Environment: The Nansen Centennial Volume*, *Geophysical Monograph Series* (Vol. 85, pp. 33–46). Washington, D. C: AGU.

Schauer, U., Fahrbach, E., Osterhus, S., & Rohardt, G. (2004). Arctic warming through the Fram Strait: Oceanic heat transport from 3 years of measurements. *Journal of Geophysical Research*, *109*, C06026. https://doi.org/10.1029/2003JC001823

Shibley, N. C., Timmermans, M.-L., Carpenter, J. R., & Toole, J. M. (2017). Spatial variability of the Arctic Ocean's double-diffusive staircase. *Journal of Geophysical Research: Oceans*, *122*, 980–994. https://doi.org/10.1002/2016JC012419

Sirevaag, A., & Fer, I. (2012). Vertical heat transfer in the Arctic Ocean: The role of double-diffusive mixing. *Journal of Geophysical Research*, *117*, C07010. https://doi.org/10.1029/2012JC007910

Steele, M., & Boyd, T. (1998). Retreat of the cold halocline layer in the Arctic Ocean. *Journal of Geophysical Research*, *103*(C5), 10,419–10,435. https://doi.org/10.1029/98JC00580

Timmermans, M.-L., Toole, J., Krishfield, R., & Winsor, P. (2008). Ice-Tethered Profiler observations of the double-diffusive staircase in the Canada Basin thermocline. *Journal of Geophysical Research*, *113*, C00A02. https://doi.org/10.1029/2008JC004829

Woodgate, R. A., Aagaard, K., Muench, R. D., Gunn, J., Bjork, G., Rudels, B., et al. (2001). The Arctic Ocean boundary current along the Eurasian slope and the adjacent Lomonosov Ridge: Water mass properties, transports and transformations from moored instruments. *Deep Sea Research*, *1*(48), 1757–1792. https://doi.org/10.1016/s0967-0637(00)00091-1